Molecular Crystals and Liquid Crystals
Publication details, including instructions for authors and subscription information:
http://www.tandfonline.com/loi/gmcl16

Paracrystalline Nature of Poly (p-Phenylene)

Akiyoshi Kawaguchi [a] & JÜRgen Petermann [b]
[a] The Institute for Chemical Research, Kyoto University, Uji, Kyoto, 611, Japan
[b] Technische Universität Hamburg-Harburg, Kunstoffverarbeitung, D2100 Hamburg 90, Schloßstraße 20, West Germany
Version of record first published: 20 Apr 2011.

To cite this article: Akiyoshi Kawaguchi & JÜRgen Petermann (1986): Paracrystalline Nature of Poly (p-Phenylene), Molecular Crystals and Liquid Crystals, 133:1-2, 189-206

To link to this article: http://dx.doi.org/10.1080/00268948608079570

Mol. Cryst. Liq. Cryst., 1986, Vol. 133, pp. 189–206
0026-8941/86/1332–0189/$20.00/0

Printed in the United States of America

Paracrystalline Nature of Poly(p-Phenylene)

AKIYOSHI KAWAGUCHI

The Institute for Chemical Research, Kyoto University, Uji, Kyoto 611, Japan

and

JÜRGEN PETERMANN

Technische Universität Hamburg-Harburg, Kunstoffverarbeitung, D2100 Hamburg 90, Schloßstraße 20, West Germany

(*Received March 27, 1985; in final form September 11, 1985*)

The electron diffraction pattern of oriented, annealed poly(p-phenylene) is explained on the basis of an orthorhombic unit cell: **a** = 0.7781, **b** = 0.5520 and **c**(fiber axis) = 0.4300 nm. and exhibits the following features:

(1) The reflections on the equator and meridian are sharp. Only a few weak diagonal reflections can be observed.
(2) Strong diffuse scattering is seen on the third layer line.
(3) The reflections on the meridian (00*l*-reflections) have a characteristic line profile, in which the intensity increases suddenly at the Bragg angle and decreases gradually.

From (1) to (3), it can be concluded that the material is paracrystalline like a nematic structure in liquid crystals. Molecular chains are laterally packed in a rather regular way. However, the disorder by the shift of chains in the direction parallel to their axes is remarkable.

Keywords: electron diffraction, poly-(p-phenylene), crystal structure, paracrystalline, shift disorder

INTRODUCTION

Poly(para-phenylene) (PPP) has been studied as one of the electrical conductive polymers, especially in the relation to doping with Lewis acids such as AsF_5 and SbF_5.[1–6] As the attention is focused on the

structural changes during the doping reaction, the crystal structure before doping has to be cleared. However, the crystal structure of this polymer is not fully explored yet.[3,7,8] In this paper the nature of the crystalline state of PPP is investigated by electron diffraction and compared with the crystal structure of its oligomers, p-quaterphenyl[9] and p-hexaphenyl.

EXPERIMENTAL

The PPP was synthesized using Kovacic's method.[7] To make the oriented films for electron microscopy, a reaction vessel comprising a double glass cylinder where the inner one is allowed to rotate was made. Dried benzene and catalyst mixture of cupric chloride and aluminum chloride were filled in between glass walls of inner and outer cylinders in an atmosphere of nitrogen. The reaction mixture was stirred by rotating the inner cylinder and then the flow was produced in the tangential direction of cylinder. As polymerization proceeded, polymers were deposited as a thin film on the wall of glass cylinder and then molecular chains were oriented in the direction of flow. The detail of the method is referred to Tieke *et al.*[4] Heat treatment of the samples was carried out in vacuum at 400°C for 24 hrs.[10] The electron microscope used here was a JEOL JEM 200 CX operated at 200 kV. For measuring the diffraction intensity, the multiple exposure method was adopted: a series of electron diffraction micrographs were recorded on KODAK SB-2 films with varying exposure times. The optical intensity of the films was measured with an optical densitometer, Joyce Loebl's Autodensidater, and converted into intensity by the standard procedure.[11]

p-Hexaphenyl, one of oligomers of PPP, was crystallized from the dilute solution in α-chloronaphthalene. The material (a product by the ICN Pharmaceuticals, Inc., USA) was dissolved in it at a temperature near its boiling point and crystallized by slow cooling.

RESULTS AND DISCUSSION

Figure 1 shows a typical electron diffraction pattern of oriented, heat treated PPP. The pattern has three remarkable features.

1) Rather sharp arcs on the equator and meridian can be seen. Only a few weak arcs are distinguishable on the second layer line,

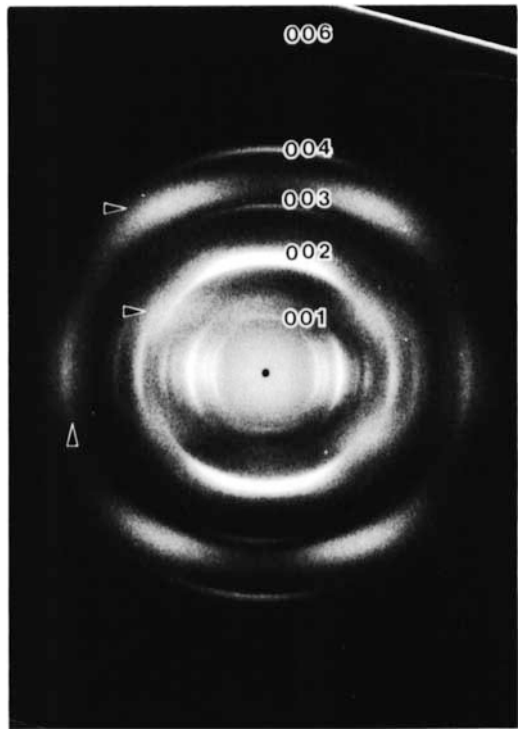

FIGURE 1 Electron diffraction pattern of annealed PPP taken at 200 kV. The molecular axis is vertical. The arrows show the characteristic diffuse scattering.

but except these, no other sharp diffraction arcs can be identified off from the equator or meridian.

2) Diffuse scattering is seen on the first, third and fifth layer lines. Most intense is the diffuse scattering on the third layer line, while that on the fifth layer line is exceedingly weak so that it is barely detectable on the heavily exposed negatives.

3) The diffraction arcs on the meridian have a characteristic profile. With increasing the diffraction angle, the intensity increases abruptly and decreases gradually.

The diffraction patterns with similar features have been observed on collagen,[12] α-keratin,[13] muscle,[14] isotactic polystyrene,[15] poly-β-propiolacton[16] and synthetic aromatic co-polyester.[17] From these diffraction features, several conclusions about the crystalline nature can be drawn.

TABLE I

The observed and calculated lattice spacings

(hkl)	annealed d_{obs} (nm)	as-polymerized d_{obs} (nm)	d_{cal} (nm)
110	0.452	0.4533	0.4502
200	0.3898	0.3991	0.3892
210	0.3176	0.3194	0.3180
020	0.276		0.276
120	0.2601		0.2607
310	0.2317		0.2348
220			0.2251
400	0.2030		0.1946
320	0.1857	0.1913	0.1890
410			0.1835
130			0.1790
420	0.1564		0.1590
330			0.1500
510			0.1490
undefined	0.1132		
001	uncertain		0.4300
002	0.2105	0.2111	0.2150
003	0.1433		0.1433
004	0.1075	0.1070	0.1075
005	not observed		0.0860
006	0.0717	0.0716	0.0716

[a]The calculation is carried out on the basis of a orthorhombic unit cell with **a** = 0.7781, **b** = 0.5520 and **c** = 0.4300 nm.

I. The crystal structure

The observed lattice spacings of as-polymerized and heat-treated samples are listed in Table I. The reflections are *tentatively* indexed on the basis of the orthorhombic unit cell with a cell dimension: **a** = 0.7781, **b** = 0.5520 and **c**(fiber axis) = 0.4300 nm. In comparison of lattice spacings between as-polymerized and heat-treated PPP, it is shown that no change in the basic crystal structure occurs during the heat treatment. As seen from the appearance of many sharp reflections, only the crystalline order increases. Till now, the repeating distance of PPP is believed to be 0.4260 nm. It has been observed that with increasing the number of monomer units within the oligomers, the repeat distance increases by the above value as an average.[18] The value was then taken as the repeat distance of the polymer. From the present analysis using the meridional reflections up to the 006 reflection, the somewhat larger value of 0.4300 nm is obtained. The distance of the structural unit of p-quaterphenyl is in perfect agreement with our value.[9]

On the equator, h00 and 0k0 diffractions with h and k odd are not observed. For comparison, electron diffractions were taken from p-hexaphenyl crystallized from the dilute solution [Figure 2]. The weak 100 and 010 spots in Figure 2 are due to the double diffraction, as they disappear in the X-ray diffraction pattern. The same extinction law in electron diffraction of the oligomer as in the polymer is observed. On the a-b projection, the cell dimension of the oligomer is very close to that of the polymer; **a** = 0.7758 nm and **b** = 0.5530 nm. From the similarity of cell dimension and extinction law, it is assumed that the oligomer and polymer have the same molecular arrangement in the unit cell. The extinction law shows that the unit cell has a 2_1 screw axis in the direction of **a** and **b** axes on the **a-b** projection: the two dimensional space group is p2gg.

From the size of the unit cell, it is assumed that two monomer units are contained in the unit cell. In consideration of the space symmetry, their arrangement on the **a-b** projection is depicted in Figure 3. The setting angle between the planes containing benzene rings and the a-axis of the unit cell is estimated at 58° by the following procedure: The observed intensity data are compared with the calculated intensities as a function of the setting angle by the Wilson method[19] and the angle at which the reliability factor

$$\mathrm{Re} = \sum ||F_{obs}(hk0)|^2 - |F_{cal}(hk0)|^2| \Big/ \sum |F_{obs}(hk0)|^2 \qquad (1)$$

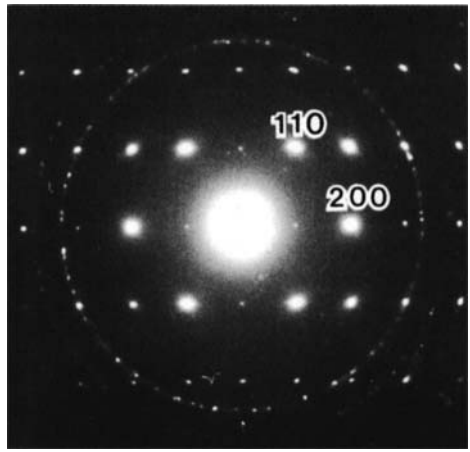

FIGURE 2 The electron diffraction pattern of a p-hexaphenyl crystal. Dotted rings shows the 111 reflection of aluminium.

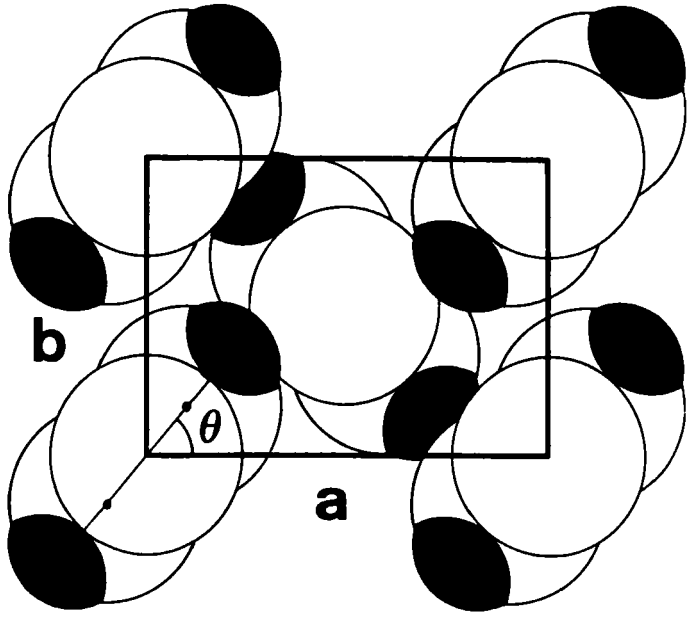

FIGURE 3 The schematic drawing of the crystal structure of PPP on the **a**-**b** projection. The **c**-axis is normal to the paper. The angle θ denotes the setting angle. Dark parts denote the hydrogen and open circles the carbon atoms.

reaches a minimum is taken as the setting angle. In the equation, $|F_{cal}(hk0)|$ and $|F_{obs}(hk0)|$ are the calculated and observed diffraction amplitudes of the hk0 reflection, respectively. In the calculation of the diffraction amplitude, it is assumed that all atoms comprising monomer units of benzene rings lie in the same plane and that their atomic coordinates are the same as in p-quaterphenyl. When all hk0 reflections are taken into account, the Re value has a shallow minimum at the setting angle of 58°. Stamm has reported the setting angle as 57°.[20] The intensity data are listed in Table II.

Previously, the lattice spacing of 0.196 nm has been indexed as the 012 reflection on the basis of the monoclinic unit cell.[3] As seen from Figure 1, no sharp, intense reflections corresponding to the 012 reflection can be identified off from the equator and meridian in our pattern.

Since information from hk*l* reflections ($l \neq 0$) is hardly obtained at the present stage, it is very difficult to construct the three dimensional crystal structure from our data. However, by comparing the observed intensities of 00*l* reflections with the calculated ones as a function of the relative shift in the above way, the most probable

TABLE II

The observed and calculated intensities

(hk0)	I_{cal}	I_{obs}
110	305	619
200	388	424
210	348	273
120	13.5	5.1
[a]310, 220	87.2	20.8
400	6.0	16.0
[a]410, 320, 130	132.3	64.4
[a]420, 330	97.4	71.4

[a] $I_{cal} = \Sigma_{hk}|F(hk0)|^2$

Re = 38% and isotropic thermal parameter = 0.05 nm^2. The accuracy of intensity measurement is assumed to be equal for all the reflections.

relative shift between the two chains in the unit cell can be obtained, because the intensities of the meridional reflections are determined only by the fractional atomic coordinates in the chain direction(c-axis). The ratio of the observed intensity of the 00l reflection to that of 002 (I(00l)/I(002)) is 2.6×10^{-2}. The ratio is attained, when the two chains in the unit cell are not on the same level but are displaced from each other by 0.193 nm (0.45 in the fractional coordinate) in the chain direction. For the present analysis, the higher order reflections ($l \geqq 3$) are meaningless, since the interference of scattering between neighboring chains is not prominent because of the large shift disorder of chains along their axes (discussed later).

On the basis of the orthorhombic unit cell, the measured 002 spacing of 0.210–0.211 nm is significantly smaller than the value expected for this structure (0.215 nm). The following reasons can be considered for this discrepancy.

1) The unit cell is orthorhombic. On the second layer line, another intense reflection (e.g. 102 or 012 reflection of this structure) is very close to the 002 reflection. These reflections overlap so that the peak position of the 002 reflection is apparently displaced to the higher diffraction angle. This would result in the observed smaller 002 spacing.

2) The unit cell is monoclinic. The small 002 spacing is due to this unit cell.

When the intensity was scanned along the 002 arc, the intensity maximum is actually measured at the azimuthal angle of 10° off from the meridian. This angle is comparable to that at which the 002

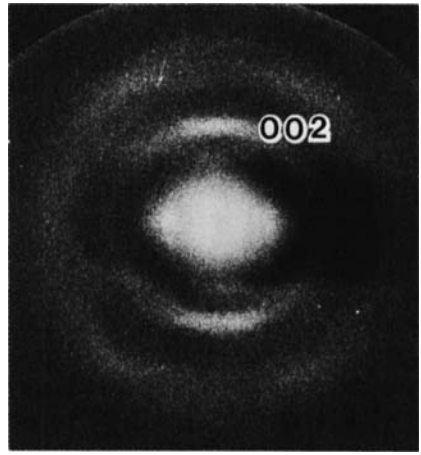

FIGURE 4 The micro-area electron diffraction pattern of PPP taken with the scanning attachment.

reflection would be expected in a fiber pattern on the basis of the monoclinic unit cell.[3,8] The larger $00l$ ($l \geqq 3$) spacings, which cannot consistently be explained on the basis of this structure, are also interpreted in terms of the default of interference in scattering between chains in disordered crystals. Thus, the possibility of the monoclinic structure cannot be ruled out uniquely. Figure 4 shows a micro-area electron diffraction pattern of PPP, which was taken from an area of 30–40 nm diameter. In the pattern, no splitting of 002 reflections can be detected, as would be expected for the monoclinic structure. From this we conclude that in PPP the orthorhombic structure is more likely.

II. The shift disorder along chains

According to the paracrystalline theory, the diffraction intensity I(s) from an object of large size can be expressed as

$$I(\mathbf{s}) = N(\langle F_u(\mathbf{s})^2\rangle - \langle F_u(\mathbf{s})\rangle^2) + N\langle F_u(\mathbf{s})\rangle^2 Z(\mathbf{s}) \qquad (2)$$

where N denotes the number of structural units in the object, $\langle F_u(\mathbf{s})\rangle$ and $\langle F_u(\mathbf{s})^2\rangle$ the scattering amplitude and intensity of a structural unit which are averaged over all units, $Z(\mathbf{s})$ the interference function and $\mathbf{s}$ the scattering vector. Thereafter, the symbol $\langle\ \rangle$ denotes the averaging operation. The distribution function of the center of gravity of the nearest neighbouring structural units plays an important role in

the theory. The functions $H_1(x_1,x_2,x_3)$, $H_2(x_1,x_2,x_3)$ and $H_3(x_1,x_2,x_3)$ denote the distribution functions in the lattice coordinates x_1,x_2 and x_3, respectively. The numbers of structural units in the x_1,x_2 and x_3 are n_1, n_2 and n_3, respectively, and then $N = n_1 \times n_2 \times n_3$. The disorder parameters of the distribution functions are specified in terms of the mean squares of the fluctuation around the average position along the respective coordinate (see Figure 6):

$$H_1; \quad \Delta_{11} \quad \Delta_{12} \quad \Delta_{13}$$

$$H_2; \quad \Delta_{21} \quad \Delta_{22} \quad \Delta_{23}$$

$$H_3; \quad \Delta_{31} \quad \Delta_{32} \quad \Delta_{33}$$

The interference function $Z_i(\mathbf{s})$ ($i = 1,2,3$), corresponding to the respective coordinate x_i, is defined and expressed in terms of the Fourier transform of the distribution function,

$$Z_i(\mathbf{s}) = \mathrm{Re}\{(1 + F_i(\mathbf{s}))/(1 + F_i(\mathbf{s}))\},$$

where $F_i(\mathbf{s})$ denotes the Fourier transform of $H_i(x_1,x_2,x_3)$ and Re means the real part of the function. Thus, the three dimensional interference function for an ideal paracrystal, where there is no correlation among the distribution functions in the respective axes, is expressed as $Z(\mathbf{s}) = Z_1(\mathbf{s})Z_2(\mathbf{s})Z_2(\mathbf{s})$.[21,22]

The crystal lattice of PPP is now redefined as depicted in Figure 5. The x_3 axis is parallel to the molecular axis. The setting of the chains alternates along the newly defined coordinates, x_1 and x_2. The orientational change of chains is neglected to ease the interpretation of lattice disorder. Figure 6 shows schematically the distribution function $H_1 - H_3$ which are set up to explain the electron diffraction pattern of PPP. The shift disorders of chains along their axes (Δ_{13} and Δ_{23}) in the x_1 and x_2 directions are to be large. The disorder parameters by displacement Δ_{11}, Δ_{12}, Δ_{21} and Δ_{22}, are small because sharp reflections with rather large h and k indices are observed. As sketched in Figure 7, the interference function $Z_1(\mathbf{s})$ largely varies with the X_3 coordinate due to the shift disorder in x_1. With the increase of X_3, the interference function spreads out in the direction of layer lines and consequently diffraction spots are broadened. Eventually, spreading is so marked on the higher layer lines that neighboring diffractions cannot be separated any more and are scattered into the

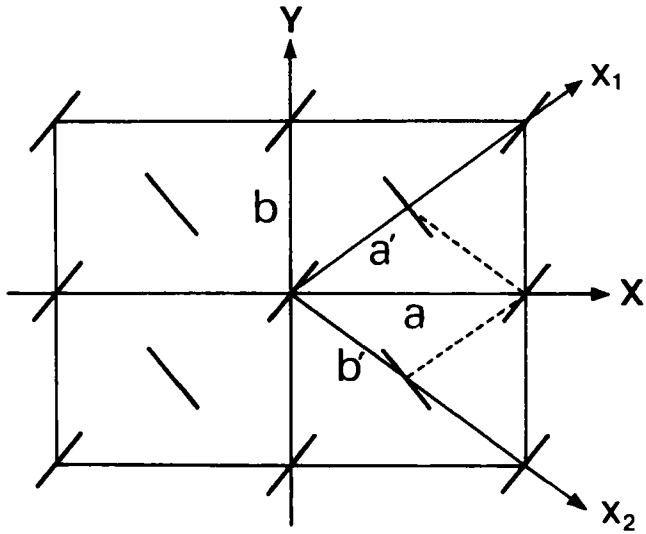

FIGURE 5 The unit cell with cell dimensions **a**′ and **b**′ is re-defined for better understanding of lattice disorder. The vectors **a** and **b** show the original unit cell. The x_1 axis is comparable to the axis and normal to the paper. Short bars indicate the projection of molecules on the **a**-**b** basal plane.

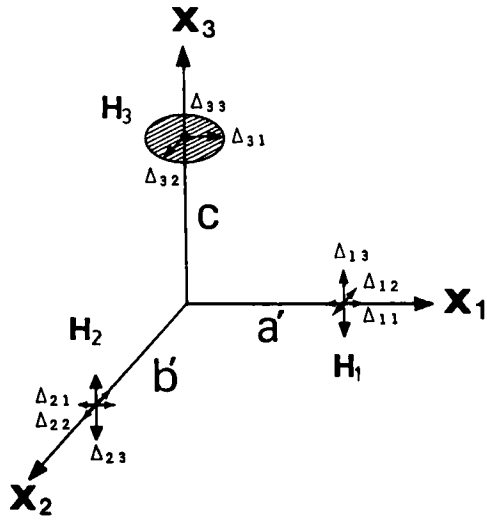

FIGURE 6 The schematic representation of the distribution functions H_1, H_2, and H_3 in real space.

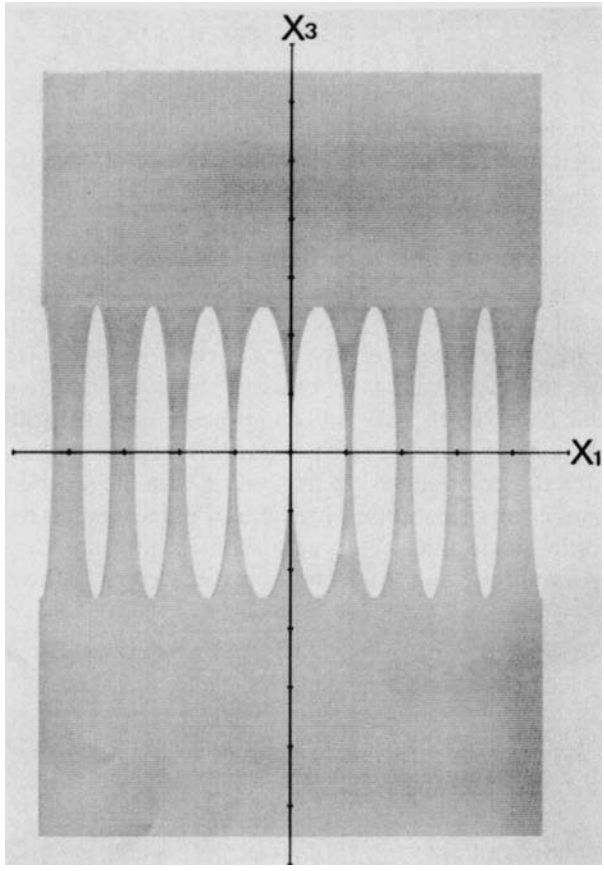

FIGURE 7 The form of interference function $Z_1(\mathbf{s})$ in $X_1 - X_3$ plane of reciprocal space produced by shift disorder Δ_{13}. The shaded area is effective. Comparable one in $X_2 - X_3$ plane is caused by the shift disorder Δ_{23}. The short lines on the meridian and equator show the unit vectors in the reciprocal lattice of the newly defined lattice.

back-ground. In such a region, the interference function $Z_1(\mathbf{s})$ changes weakly with $\mathbf{s}$, fluctuating around unity: $Z_1(\mathbf{s}) \cong 1$. The same proposition $Z_2(\mathbf{s}) \cong 1$ results from the shift disorder of Δ_{23}. Thus, the scattering intensity $I(\mathbf{s})$ is $N'I_M(\mathbf{s})$, where $I_M(\mathbf{s})$ denotes the scattering intensity of a molecule and N' $(= n_1 \times n_2)$ the number of molecules. The scattering intensity of a single molecule is easily derived from Eq. (2) as:

$$I_M(\mathbf{s}) = n_3(\langle F_u(\mathbf{s})^2\rangle - \langle F_u(\mathbf{s})\rangle^2) + n_3\langle F_u(\mathbf{s})\rangle^2 Z_3(\mathbf{s}) \qquad (3)$$

where n_3 is the number of structural units in a single molecule and

averaging is taken over all structural units of a single molecule. This means that, when the interference in intermolecular scattering is not effective, the scattering itself behaves as from a single chain.

It is assumed that the structural units, i.e. the benzene rings, are not arranged in a coplanar way along the molecular axis. They could deviate slightly from the planar conformation by random twisting around the molecular axis. In a specimen, however, the rotational symmetry around its fiber axis holds. Thus, even though a single molecule has no rotational symmetry, the symmetry is produced by averaging all orientation of structural units over the whole specimen. Conveniently, the scattering of the system with such a rotational symmetry can be explained in terms of the cylindrical coordinates (r,z,ψ) and (R,Z,Ψ) in real and reciprocal space, respectively. As usual, z and Z are parallel to the molecular axis, r and R the radii and ψ and Ψ the polar angles. In the system with the radial symmetry, averaging over all orientation of structural units is equal to that with respect to the polar angle Ψ in reciprocal space. Thus, the averaged scattering amplitude and intensity are expressed as follows:[22]

$$\langle F(R,Z,\Psi)\rangle_{\Psi} = \sum_i f_i J_0(2\pi r_i R) \exp(-2\pi i z_i Z) \tag{4}$$

where f_i, r_i and z_i are the atomic scattering factor, radius and height of the i-th atom, and

$$\langle F(R,Z,\Psi)^2\rangle_{\Psi} = \sum_i \sum_j f_i f_j J_0(2\pi r_{ij} R) \exp(-2\pi i z_{ij} Z) \tag{5}$$

where f_i and f_j are the atomic scattering factors of the i- and j-th atoms, r_{ij} and z_{ij} are the distances between the two atoms in r and z coordinates, respectively. J_0 is the Bessel function of the zeroth order. The structural unit of PPP is the benzene ring of the repeating unit. The intensity distribution was computed for 200 kV electrons using Eqs. (3), (4) and (5). In the computation, the configuration of the benzene ring analysed by Pelugeard *et al*[9] was used. Figure 8 shows the electron diffraction patterns computed for the different numbers of repeating unit. The diffuse arcs on the first, third and fifth layer lines and the undefined broad maximum on the equator are clearly reproduced. With the increase of the number of repeat units, the diffraction pattern becomes sharper. Apparently, the appearance of the pattern for a larger number of units is quite different from that of the observed pattern. However, the pattern similar to the observed

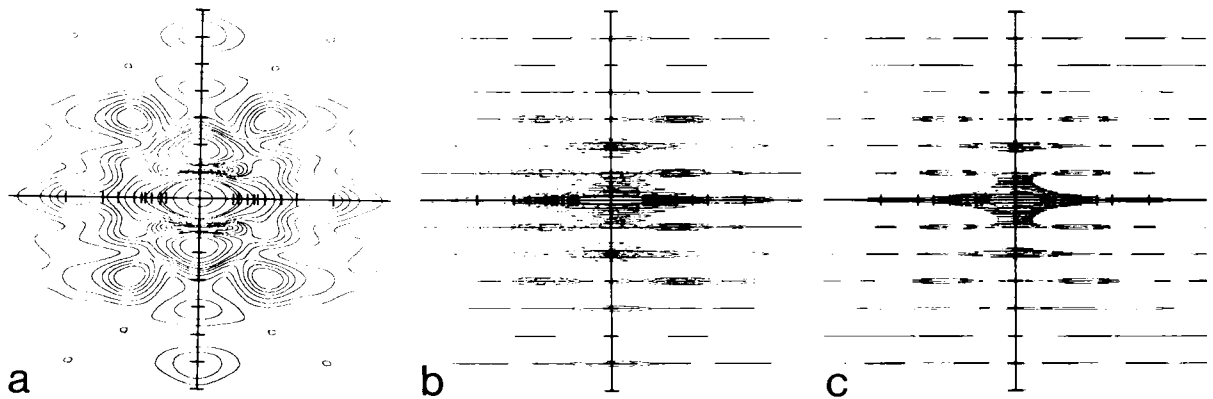

FIGURE 8 The computed intensity distribution. The number of repeating units (n_3) and the intensity levels of the contour maps from the outside are as follows: (a) n_3 = 1 and the levels are 1.,2.,4.,6.,8.,10.,15.,20.,30.,50.,80.,100.,200. and 400. A^2, respectively, (b) n_3 = 6 and the levels are 6.,20.,50.,100.,200. and 400. A^2, and (c) n_3 = 20 and the levels are 5.,20. and 100. A^2. The short bars on the meridian and equator show the the positions corresponding to the observed reflections. The fiber axis is vertical.

is easily produced by distributing the computed pattern around the Z axis. By comparing the observed and computed patterns, it is proved that the diffuse scattering is caused by the shift disorder and by the incoherently aligned benzene rings.

In the electron diffraction pattern, there is no sharp crystalline reflection on the layer lines with $l \geqq 3$. This shows that the third layer line is the boundary over which the interference in intermolecular scattering is ineffective and the crystalline scattering transfers into the diffused. As described above, this is the reason why the meridional reflections ($l \geqq 3$) cannot be used to estimate the "relative shift between two chains in the unit cell" and their spacings are no longer dependent on the crystal form. According to Hosemann's criterion, assuming the Gaussian function for H_i, the limiting boundary index l at which the transition from the crystalline to diffuse scattering occurs is given by $l = 0.25\ c/\Delta_{ij}$, where c is the lattice constant.[21,22] When this expression is applied to the third layer line, the disorder parameter Δ_{13} ($\cong \Delta_{23}$) is obtained at 0.04 nm.

Using the above analysis only, it cannot be fully explained that no sharp, crystalline reflection is observed on layer lines below the second. As seen on the equator in Figure 1, the hk0 reflections at the large scattering angles are too broad to distinguish them from the diffuse scattering by single molecules. This shows that due to displacement disorders in the x_1 and x_2 directions, the interference functions $Z_1(\mathbf{s})$ and $Z_2(\mathbf{s})$ spread so largely that the reflections spread into a diffuse scattering. By taking account of spreading of $Z_3(\mathbf{s})$ due to the disorders in the x_3 axis (Δ_{31} and Δ_{32}), it is explained qualitatively that the total interference function $Z(\mathbf{s})$ spreads further and that the crystalline reflections even on the layer lines below the second is broadened into the diffuse background. Anyhow, it is stressed here that in PPP the shift disorder in the molecular axis is very remarkable.

III. The rigid conformation

As sharp meridional reflections can be observed up to the 006 reflection, the chains have a "rigid conformation" in which the structural units are regularly ordered in the direction of the molecular axis. This means that the disorder parameter Δ_{33} is very small. Even on the heavily exposed negatives, no 005 reflection is observed. As lined out in section II, the interference of intermolecular scattering does not affect the reflections higher than the third layer line, that is, these are caused only by single chains. The conformation of a single chain is responsible for the extinction of the 005 reflection.

The 005 reflection was assumed to be extinct, when its intensity was reduced to 1% of that of the 006 reflection. The chain conformation was probed with a computer simulation in such a way as z-coordinates of hydrogen and carbon atoms were varied to fulfill the above condition. It is evident from the atomic scattering factors that the reflection intensity largely depends on the position of carbon atoms. From z-coordinates thus derived, the C_1—C_1' bond length is evaluated at 0.149 nm and the C_2—C_3 bond length in the benzene ring at 0.14–0.142 nm (see Figure 9). These values are in good agreement with those of p-quaterphenyl. The model used above to estimate diffraction intensities is found to be reasonable.

It has been shown by Jones[23] and Deas[24] that the linear gratings distributed randomly in real space exhibit a characteristic diffraction profile: with the increase of the scattering angle, the diffraction intensity increases sharply at a given angle and decreases gradually tailing off. The diffraction feature is clearly realized in the diffraction profile of the meridional reflections, as observed in Figure 1. They have a sharp edge at the side of lower angle and there their intensity increases abruptly and decreases gradually with increasing the diffraction angle. The shape and sharpness of the profile is largely de-

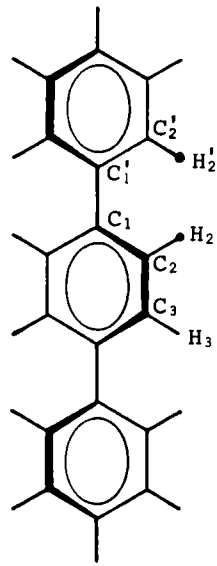

FIGURE 9 The favorable conformation of a PPP chain, which is not planar due to the steric hindrance between neighbouring hydrogens, H_2 and H_2'. The thick lines indicate their direction is upwards out of the surface of paper.

pendent on the number of repeat units in a chain and on the degree of orientation of chains in the specimen. When the orientation function is known, the number of repeat units in a molecule can be estimated in comparison of the computed and observed curves and *vice versa*. However, the measured profile is not accurate enough to give quantitative analysis of the number of units per molecule. Anyhow, the PPP molecular chain is rigid and linear enough to be considered as a linear grating, as the line profile of the meridional reflections possesses the features expected for the grating.

CONCLUDING REMARKS

Single chains may have the chemically irregular structural units such as orth- or meta-configuration. When such chains are incorporated in the crystal lattice, the lattice is largely distorted around irregular components and chains surrounding them are possibly bent. Since the configurational analysis was not carried out, the origin of disorder of PPP can not be made clear. The chemical disorder of a single chain is surely one of possible causes for the lattice distortion. Further, it is to be noted that PPP specimen prepared in the present method is polydispersed containing the low molecular weight species and that the structure of chain ends is not defined but is random.[25,26] When such a whole polymer is crystallized, the chain ends of random structure might be incorporated in crystals and consequently the distortion or disorder of the crystal lattice could be caused.

Even if the PPP chains completely comprise the structural units in the para-configuration, they could not be planar and take an irregular conformation. Since repulsion between hydrogen atoms protruding from the neighbouring benzene rings, H_2—H_2', is serious, the molecular chains must be twisted around the bond C_2—C_2' to reduce the steric hindrance (see Figure 9). The high temperature phase of p-phenylene oligomers typically evidences this kind of disorder in the direction of rotation between neighbouring phenyl rings. An "averaged" planar structure without disorder in the position of chain center is produced, because the rings move in the double potential well whose minima are located on either side of coplanar conformation.[9,27] On the same origin as this, analogous disorder of chain conformation is expected in poly(p-phenylene). Benzene rings along the PPP chain twist clockwise or anticlockwise around the molecular axis with equal probability statistically so that they could settle in a energetically favorite position deviated from the planar structure. Even though the

orientation of the benzene rings changes thus randomly, a chain still keeps firmly the regularity of the atomic position in the direction chain axis and has a planar conformation as an average. If the distance between neighbouring chains is sufficiently large, such "averaged" planar chains could be packed side-by-side keeping the distance between neighbours fixed. However, as their conformation is irregular, the chains may not be settled in a regular position in the direction of their axes and then the three-dimensional order may be lost. Thus, the nematic structure observed in liquid crystals could be caused by this conformational irregularity.

Acknowledgment

This work was carried out at the University of Saarland, while A.K. was staying in the Germany Federal Republic. We are grateful to the Volkswagen Foundation for the financial support and are indebted to Prof. H. Gleiter of the Univ. of Saarland for his encouragement during performance of this work, to Dr. S. Isoda of Kyoto Univ. for his help in optical densitometry and to Dr. B. Tieke and Prof. G. Wegner of Freiburg Univ. for their help to prepare specimens.

References

1. L. W. Shacklette, R. R. Chance, D. M. Ivory, G. G. Miller and R. H. Baughmann, *Synth. Met.*, **1**, 307 (1980).
2. M. Stamm, J. Hocker and A. Axmann, *Mol. Cryst. Liq. Cryst.*, **77**, 125 (1981).
3. H. W. Hasslin and C. Riekel, *Synth. Met.*, **5**, 37 (1982).
4. B. Tieke, C. Bubeck and G. Lieser, *Makromol. Chem., Rapid. Commun.*, **3**, 261 (1982).
5. B. Tieke, C. Bubeck and G. Lieser, *J. de Physique*, Coll. C3, **44**, 753 (1983).
6. M. Stamm, *Mol. Cryst. Liq. Cryst.*, **105**, 259 (1984).
7. P. Kovacic, M. B. Feldman, J. P. Kovacic and J. B. Lando, *J. Appl. Polym. Sci.*, **12**, 1735 (1968).
8. F. Teraoka and T. Takahashi, *J. Macromol. Sci. -Phys.*, **B18(1)**, 73 (1980).
9. Y. Delugeard, J. Desuche and J. L. Baudour, *Acta Cryst.*, **B32**, 702 (1976).
10. G. Froyer, F. Maurice, J. P. Mercier, D. Riviere, M. LeCun and P. Auvray, *Polymer*, **22**, 992 (1981).
11. B. K. Vainshtein, *Structure Analysis by Electron Diffraction* (Pergamon Press, London 1964).
12. A. Rich and F. H. C. Crick, *Nature*, **176**, 593 (1955).
13. R. S. Bear and H. F. Rugo, *Ann. N. Y. Acad. Sci.*, **53**, 627 (1951).
14. C. Cohen and K. C. Holmes, *J. Mol. Biol.*, **6**, 423 (1963).
15. E. D. T. Atkins, D. H. Issac, A. Keller and K. Miyasaka, *J. Polymer Sci. Polymer Phys. Ed.*, **15**, 211 (1977).
16. K. Suehiro, Y. Chatani and H. Tadokoro, *Polymer J.*, **7**, 352 (1975).
17. J. Blackwell and G. Gutierrez, *Polymer*, **23**, 671 (1982).
18. C. J. Toussaint, *Acta Cryst.*, **21**, 1002 (1966).
19. A. J. C. Wilson, *Acta Cryst.*, **2**, 378 (1949).

20. M. Stamm, *Ferienkurs '84, Neutronenstreuung fur Physik und Chemie der kondensieten Materie und fur Molecularbiologie*, (WEKA-DRUCK, Linnick, 1984).
21. R. Hosemann and S. N. Bagchi, *Direct analysis of diffraction by matter* (North Holland, Amsterdam, 1962).
22. B. K. Vainshtein, *Diffraction of X-rays by chain molecules* (Elsevier, London, 1964).
23. R. C. Jones, *Acta Cryst.*, **2**, 252 (1948).
24. H. D. Deas, *Acta Cryst.*, **5**, 542 (1952).
25. P. Kovacic, J. T. Uchic and L-C Hsu, *J. Polymer Sci.*, Part A-1, **5**, 945 (1967).
26. L. W. Schaklette, H. Eckhardt, R. R. Chance, G. G. Miller, D. M. Ivory and R. H. Baughman, *J. Chem. Phys.*, **73**, 4098 (1980).
27. G. M. Parkinson, W. Jones and J. M. Thomas, *Electron Microscopy at Molecular Dimensions* (Springer Verlag, Berlin, 1980), ed by W. Braumeister and W. Vogell, pp. 208–225.